Excerpt from the Proceedings of the 2011 COMSOL Conference in Boston

Modeling Non-linear Plasma-wave Interaction at the Edge of a Tokamak Plasma

O. Meneghini*, S. Shiraiwa, C. Lau, I. Faust, B. LaBombard, G. Wallace, R. Parker, R. Wilson†, S. Wukitch and the Alcator C-Mod team
Massachusetts Institute of Technology - Plasma Science and Fusion Center
† Princeton Plasma Physics Laboratory
* Corresponding author: 77 Massachusetts Ave., Cambridge, MA ; orso@mit.edu

Abstract: High power RF waves interact strongly with the edge of Tokamak plasmas by means of ponderomotive forces. This phenomenon results in a depletion of the density where the wave fields are high and affects the wave propagation itself, thus making the overall problem non-linear. On the Alcator C-Mod tokamak, edge density profile measurements by means of an X-mode Scrape Off Layer reflectometer were able for the first time to accurately document the density depletion profile in the presence of high power LHRF. The measured reflection coefficients and density profiles were well reproduced by means of a fullwave COMSOL simulation in which the density depletion by ponderomotive forces is self-consistently taken into account via an iterative approach.

Keywords: plasma, wave, electromagnetic, Lower Hybrid, tokamak

1. Introduction

Tokamak experiments have show that the linear theory of lower hybrid (LH) waveguide coupling begins to break down if the radio frequency (RF) power flux exceeds approximately 0.3 MW/m^2. In this regime the high power RF waves interact strongly and modify the edge plasma which in turns affect the wave propagation itself, thus making the overall problem non-linear. Even though all current drive experiments ultimately operate at high power, the wave coupling in the non-linear regime is still poorly understood and a definitive theoretical model is missing. Experimental evidence and modeling have pointed to ponderomotive forces as the leading candidate to explain this observation. Ponderomotive forces push charged particles that are in an inhomogeneous oscillating electromagnetic field towards the weaker field areas. In a plasma this results in a depletion of the density where the wave fields are high. On the Alcator C-Mod tokamak, the LH wave coupling at high power (>1 MW/m^2) was observed to degrade for higher launched phasing, suggesting that the waves have to tunnel through a millimetric evanescent layer between the plasma and the launcher. Subsequent edge density profile measurements by means of an X- mode Scrape Off Layer (SOL) reflectometer were able for the first time to accurately document the density depletion profile in the presence of high power LHRF. Good coupling was recovered for non-perturbative power level experiments (few Watts), confirming the role of high power LHRF waves on the edge plasma profiles. The measured reflection coefficients and density profiles were well reproduced by means of a fullwave COMSOL simulation in which the density depletion by ponderomotive forces is self-consistently taken into account via an iterative approach. This model has been verified with previous 1-D calculations and has been seamlessly extended to efficiently model arbitrary 2-D or 3-D geometries. We found that considering a realistic geometry further exacerbates the density depletion in front of the launcher and is a key ingredient to get good agreement with the reflectometer measurements.

2. Lower Hybrid wave coupling

Linear coupling theory for Lower Hybrid waves [1] has been validated in several experiments but has been shown to break down at high power densities.

Lower Hybrid coupling strongly depends on the details of the density profile at the mouth of the antenna and common practice has been to use the ambiguity of the edge density profile to fit coupling simulations to the experimental measurements. As an example, consider that the density profile in front of the LH grill is typically modeled by a density profile of the form:

$$\mathrm{n}_e = \begin{cases} n_{e0} + \frac{\mathrm{d}n}{\mathrm{d}x}(x - \Delta_{GAP}) & \text{, if } x \geq \Delta_{GAP} \\ 0 & \text{, if } x < \Delta_{GAP} \end{cases}$$

where the antenna is assumed to be at x=0, n_{e0} is the density pedestal, dn/dx is the density

gradient, and Δ_{GAP} is a vacuum region between the launcher and the plasma. This type of profile was first proposed in Ref. [3] and analyzed in detail in Ref. [4]. A graphical representation of such a profile is shown in Fig. 1.

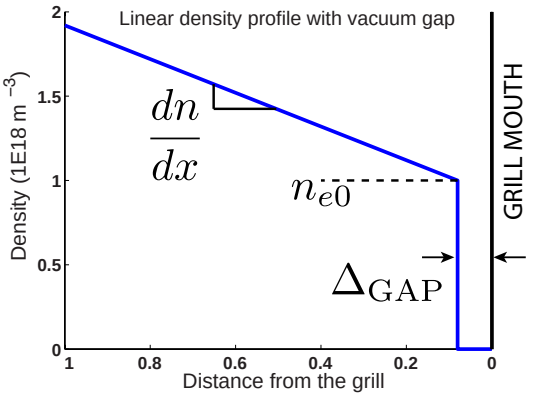

Figure 1. Linear density profile commonly used in Lower Hybrid coupling simulation codes.

The presence of this gap has never been measured, and different theories have been put forward to justify its possible existence. These include: modification of the transport phenomena during LH [5], misalignment of the grill [6], limiter shadowing in front of the waveguides or an improper match between plasma and grill curvature [6]. However, the most plausible cause is that the plasma is pushed away under the action of ponderomotive forces acting on the plasma surface [3, 4, 7, 8], resulting in an effective shift of the density profile in the radial direction, thus creating a low density region where LH waves are evanescent and increasing the reflection coefficient. It is clear that a definitive theoretical model in this regime is still missing; experimental observations are often contradictory and additional experimental information is therefore essential.

The Alcator C-Mod LH launcher is in a unique position to study LH wave coupling. In fact the LH launcher is not only equipped with three sets of two Langmuir probes of different lengths, but also has an X-mode SOL reflectometer to measure the actual density profile in front of the launcher at three poloidal locations. The availability of accurate density profile measurements eliminates these free parameters and enable a characterization of the antenna coupling performance and a self-consistent validation of LH wave coupling codes. In this paper we found that the experimental results support the existence of a density depletion in the presence of high power RF and modeling showed that this is compatible with what is expected by ponderomotive forces.

3. **High power coupling on Alcator C-Mod**

On the Alcator C-Mod tokamak, although the average reflection coefficient measured during high power operations (>1~MW/m^2) at the input of the splitters can be reduced to be as low as ~15% in optimized conditions, its amplitude is usually higher than simulations predicted at the design stage for typical SOL density parameters [9]. To address this issue, a systematic survey of the coupling properties of the launcher has been carried out. This result is shown in Fig. 2, where the power reflection coefficient is plot as a function of average edge density as measured by the Langmuir probes embedded into the LH antenna. In this figure, two discharges are presented, one with the launcher being δ=0.1 mm behind the protecting limiter, the other for δ=1 mm. In these experiments the plasma equilibrium was kept constant while the density was swept during the LH pulse by gas puffing.

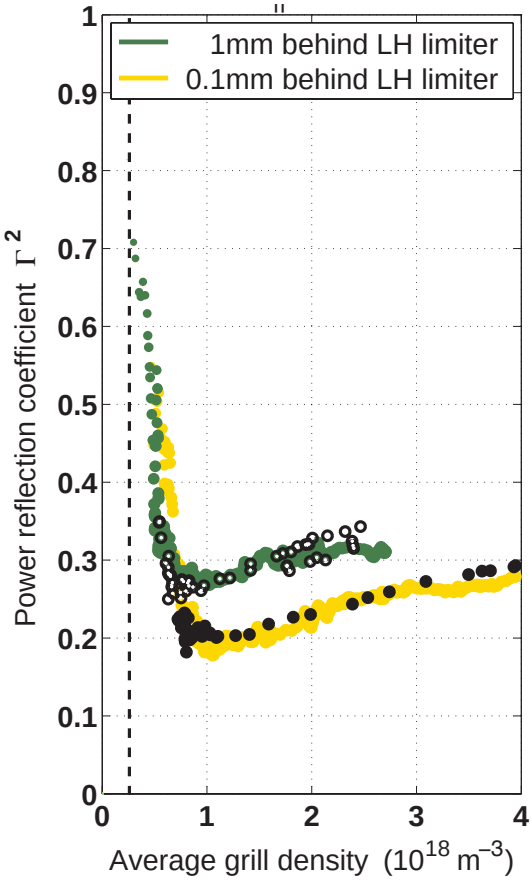

Figure 2. Power reflection coefficient as a function of average probe density for different phasing and launcher radial positions behind the private

limiters. The filled black circles and the open black circles are coupling simulations using the Brambilla code and the density model with variable gap.

In this experiment, the measurements of the power reflection coefficient shows the typical trend predicted by linear coupling theory [1], the reflections rapidly increasing for densities close to the cutoff density and reaching a minimum, which is more pronounced at lower phasing. Interestingly, the reflection coefficient is observed to increase at higher phasing, suggesting that the waves tunnel through an evanescent layer. Also, reflections are systematically lower when the launcher is pushed farther towards the plasma.

LH wave coupling simulations have been carried out using the density measurements from the Langmuir probes installed in front of the launcher. A wide range of experimental observations were reproduced with the GRILL code [1] (filled black circles and the open black circles in Fig. 2), provided that the density profiles included the presence of a vacuum gap of the order of 1 mm. The density at the coupler is measured by the Langmuir probes while the density gradient is estimated by taking the edge-most channel of the Thomson scattering system. This density model is supported by the observation that the reflection coefficient is observed to increase at higher phasing, suggesting that the waves tunnel through an evanescent region. However, it was not possible to reproduce the experimental measurements using a single vacuum gap value across the whole density scan. Hence, a new variable density gap was used:

$$\Delta_{GAP} = \Delta_{GAP0}(1 - \alpha\, n_{e0})$$

The idea behind this model is that the vacuum gap reduces proportionally as the edge density increases. The parameters Δ_{GAP0} and α were chosen so to best reproduce the experimental measurements and were found to be Δ_{GAP0}=1 mm for δ=0.1 mm and Δ_{GAP0} = 1.3 mm for δ=1 mm. In both cases α=2x10^{-20} m^3. This model is an extension of the model which has been used so far to explain LH wave coupling on several machines [3, 4].

As previously mentioned, the inclusion of a vacuum gap has been widely used to explain LH wave coupling on several machines. However, the presence of this gap has never been measured and its existence often questioned. On Alcator C-Mod for the first time the depletion of the density profile in front of the launcher was directly measured with the SOL X-mode reflectometer diagnostic [10, 11]. A density depletion is observed within the first few mm away from the grill mouth, while farther inside of the plasma the density increases, possibly due to RF-induced ionization or convective cell formation.

3. Density measurements by SOL X-mode reflectometer and Langmuir probes

For the first time the density depletion induced by high power LH waves was measured by SOL X-mode reflectometer. Such an effect is best evident for LH power modulation experiments as reported in Fig. 3. The Langmuir probes also register a reduction of the electron density and an increase of the electron temperature. The latter is of particular interest because the temperature increase can act as an important feedback mechanism for ponderomotive effects.

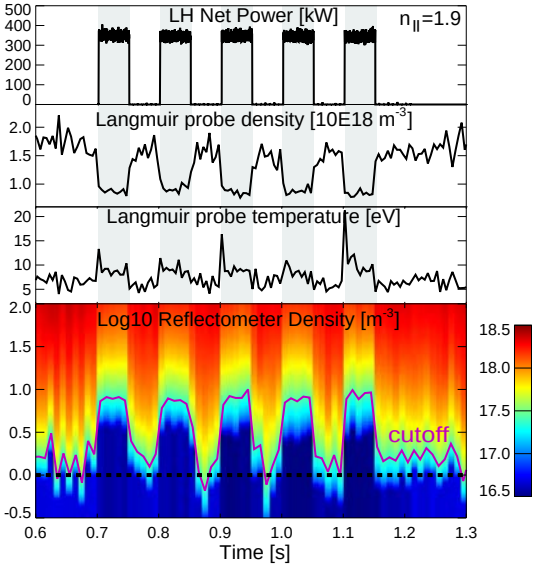

Figure 3. SOL measurements during a LH power modulation experiment (core density n_e=0.8x10^{20} m^{-3}). This type of experiment has been used to generate the average density profiles presented in Figure 4.

The following study focuses on three power modulation experiments which have three different line averaged densities. The SOL density profiles are reported in Fig. 4. These are spline fits to the data collected during the *LH on* and *LH off* periods of the modulation experiment; thus allows an increase in the measurement statistics. From the measurements it is immediately clear that a density depletion by LH waves in the very proximity of the launcher

is always present. These profiles are also in qualitative agreement with the variable gap model that was introduced in the previous section. From these profiles one can also observe that the density tends to rise about 2 cm away from the launcher.

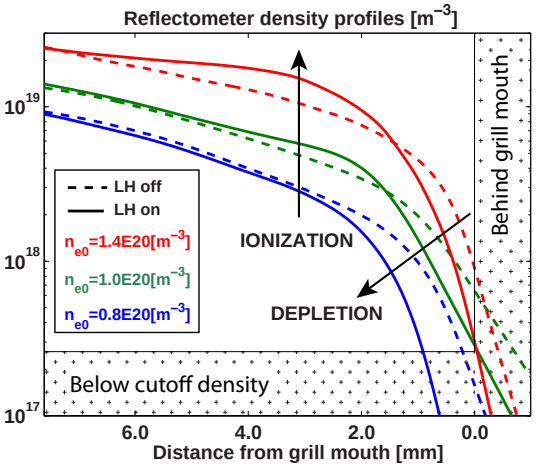

Figure 4. Density profiles measured by reflectometer for core densities of n_e=0.8x10^{20} m^{-3}, n_e=1.0x10^{20} m^{-3} and n_e=1.4x10^{20} m^{-3}. Solid and dashed lines represent the profiles in presence and absence of high power LH waves, respectively.

In general, in presence of high power LH waves the SOL exhibits 3D structures which are apparent when looking at the LH launcher with a visible camera. Figure 5 shows glowing striations which are routinely observed above waveguide rows during high power operation. This 3D structure is also confirmed by the Langmuir probe measurements. In particular, Ref. [12] attributed a similar observation on ASDEX to the formation of vortices (or convective cells) in front of the plasma [13]. Although there is clear experimental evidence of these convective cells and numerical tools such as COMSOL allow the description of arbitrary 3D non-uniformities of the plasma parameters, for the time being we retain these vortices as a second order effect and assume that the plasma is an infinite slab medium allowing only variations in the radial direction.

2D coupling simulations using the reflectometer density profiles reported in Fig. 4 were performed using COMSOL and the results are reported in the following Table:

	0.8E20	1.0E20	1.4E20
Experiment	29%	29%	28%
Simulation	34%	27%	30%
Sim. OH phase	20%	11%	10%

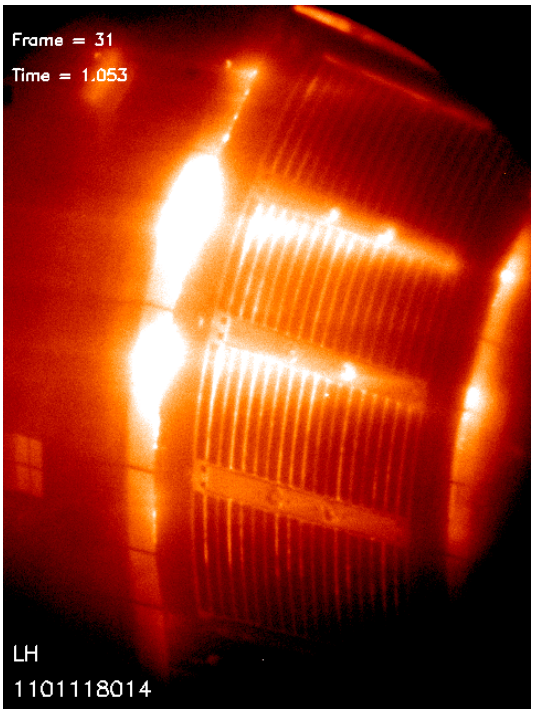

Figure 5. Visible camera frame, showing glowing striations (aligned along the magnetic field lines) which are routinely observed above waveguide rows during high power operation.

The simulated reflection coefficients are found to be more sensitive to the details of the profiles than what has been actually measured. Nonetheless, simulations were found to agree within a few percent of the experimental measurements, that is quite remarkable considering that the 3D structure of the SOL and of the launcher was completely neglected. For reference, simulations were run also for the ohmic profiles (i.e. when LH was off). In this case the reflection coefficients were found to be systematically lower. Comparing the simulation results for *LH on* and *LH off*, suggests that both a low density at the grill (especially in the presence of an evanescent layer) and a steep density gradient contribute negatively to the wave coupling.

A word of caution has to be said regarding the calibration of the reflectometer profiles. This in fact relies on the EFIT magnetic equilibrium reconstruction to locate the position of the X-Mode cutoff, which is used as the starting point for the inversion of the raw data. Errors in the magnetic field of the order of 0.1% result in errors of the order of 1 mm in the radial location of the reflectometer profiles. This is by far the largest uncertainly in this system. By comparison the shape of the profile is instead a robust quantity. To reduce this uncertainty the

measurements by the Langmuir probes have been used to constrain the radial shift of the measured reflectometer profiles. Although the length of the Langmuir probes is of the order of a mm and therefore it does not necessarily reduce the absolute error in the shift of the profiles, the same consistent assumption has been done for all of the measurements presented in this paper.

4. Use of COMSOL Multiphysics: modeling of SOL modification by ponderomotive forces

Ponderomotive force is the force that charged particles experience in an inhomogeneous oscillating field which makes them drift toward the weaker field area. To evaluate the effect on the plasma density it is advantageous to introduce the concept of a ponderomotive potential ϕ_P (defined as $\mathbf{F}_P=-\nabla\phi_P$ where $\mathbf{F}_P$ is the ponderomotive force). At equilibrium the density of each species follows the Boltzmann distribution and ϕ_P has to balance the electrostatic potential ϕ_{cs} which is due to charge separation:

$$n=n_0 \exp\left(-\frac{e(\Phi_{cs}+\Phi_P)}{\kappa T}\right)$$

In theory ponderomotive force acts on all species in the plasma, also on the ions, however in view of the inverse proportionality to the mass of the particle, this effect is mostly relevant for electrons. Imposing quasi-neutrality eliminates ϕ_{cs} and, for small deviations from the equilibrium density n_{e0}, one can expand the electron particle density as $n_e \sim n_{e0}(1+\delta n)$, where

$$\delta n = -\frac{e(\Phi_{Pe}+\Phi_{Pi})}{\kappa(T_e+T_i)}$$

The ponderomotive potential ϕ_P for a uniform magnetized cold plasma has been derived derived in Ref. [15], based on the Hamiltonian of the particles oscillation center in an electromagnetic wave field gives as a result:

$$\Phi_P = \frac{e}{m}\left[\frac{|E_z|^2}{\omega^2}+\frac{|E_x|^2+|E_y|^2}{\omega^2-\Omega^2}+ + \mathrm{Im}\left\{\frac{\Omega(E_y * Ex - E_x * E_y)}{\omega(\omega^2-\Omega^2)}\right\}\right]$$

where it is assumed that the static magnetic field $\mathbf{B}=B_0\hat{z}$. Worth pointing out is that the net effect of the wave fields on the plasma density depends on the ratio of the ponderomotive to the kinetic potential. The plasma temperature can be an important feedback mechanism for ponderomotive effects, since the injection of high power RF waves also tends to heat the plasma in the vicinity of the launcher through collisional damping.

The density perturbation and wave propagation are coupled to one another in a non-linear way (the former depends on the wave fields and the latter depends on the dielectric tensor which is a function of the plasma density). Following the derivation from [3], the analytical formulation of the non-linear problem employs the conventional cold plasma wave equation where the density is modified by the ponderomotive potential. To find an analytic solution to the problem, previous work have made further simplifying assumptions like considering only 1D geometries, slow wave propagation and assuming a monochromatic wave spectrum [13, 3, 7]. For our analysis instead, the solution was found by means of a fullwave finite element method (FEM) simulation in which the non linear coupling between the wave electric fields and the density depletion by ponderomotive forces is taken into account via an iterative approach. The new code has been named POND.

4.1 The POND code

POND solves the non-linear problem via the iterative approach depicted in Fig. 6. To start, the wave electric field is calculated from the radial density profile in absence of the LH waves. The density perturbation is then calculated. The resulting radial density profile is then used for the new iteration step until the solution converges. POND has been verified in 1D against the results published in Ref. [14]. In particular the density profile modification as a function of power was well reproduced, as show in Fig. 7.

As we shall see, the overlapping of the LH resonance cones produces a 2D structure of the density depletion in front of the grill. In the experiment, one can expect the 2D structure of the density depletion to be blurred out by the effect of parallel particle transport, the perpendicular transport being assumed to be much smaller. In other words, one can expect electrons to travel across the grill in the time period of few wave oscillations. In the following study the density along the magnetic field line is assumed to be constant and equal to the average of the density along the magnetic field lines. This is not a limitation of the code itself (which

allows the density to be specified arbitrarily at any point in space) but rather a simplifying assumption that avoids the problem of trying to pin down an accurate value for the parallel and perpendicular particle transport.

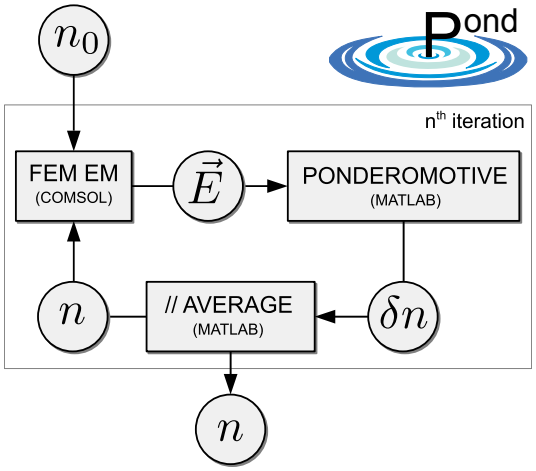

Figure 6. The POND procedure starts from the density profile in absence of LH waves and iterates until the wave fields and the perturbed density profile reach equilibrium. For the calculating the electromagnetic wave fields in the plasma COMSOL Multiphysics has been used. The main advantage of using a FEM scheme is the possibility of seamlessly extending the numerical simulations to 2D or even 3D. Differently from spectral approaches, FEM allow the electron density to be uniquely specified at any point in space thus allowing for the description of complicated geometries or non-uniformities in the plasma. Also, the FEM approach implemented is generic, efficient and scalable.

It is worth pointing out that the POND code is very generic and relies only on the assumption that the wave power is of the same order of the temperature. Hence, even if in the following we restrict our analysis to LH waves, this method could in principle be used to investigate the effect of ponderomotive forces in other frequency ranges.

4.2 Validation of POND with the Alcator C-Mod experiment

Using this exact same model the modification of the density profiles as measured on Alcator C-Mod was simulated. Starting from the density profile measured by reflectometer during ohmic phase, the density perturbation by ponderomotive forces was calculated and compared with the density profile measured by reflectometer during lower hybrid phase. Worth pointing is that the number of free parameters in this validation process is very limited. In the model, the LH net power density is set to be equal to average value in the experiment. The temperature is set to decay exponentially from 70 eV at the separatrix to the temperature measured by Langmuir probes at the edge.

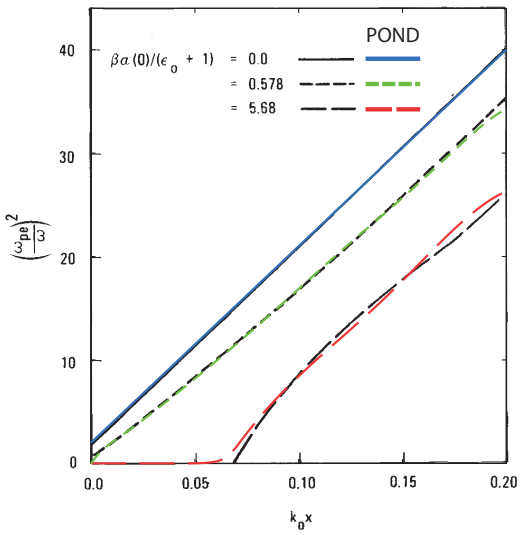

Figure 7. Comparison of the FEM approach with results from Ref. [14]. In this simulation only a single spectral component $n_{||}$=10 is considered, only slow wave is present (both its electromagnetic and electrostatic components), T_e=10 eV, T_i~0 and 2 power levels are compared: 6 kW, 60 kW. The starting density profile is linear. Everything has been normalized to the same units of Ref. [14] to allow over-plotting.

The simulation results are shown in Fig. 8 as black traces. By comparing the modeling results to the experimental density profiles at the very edge of the plasma, one can state that these are consistent with the theory of ponderomotive forces being the cause of the density depletion measured in front of the launcher. The density depletion model used in POND allows only for the density to be reduced by the presence of the ponderomotive potential. The increase of density which is observed in the experiment cannot be reproduced by this model and additional processes must be included in the model.

As previously stated, the main advantage of using a FEM approach is that the same formulation can be seamlessly applied to more complicated geometries and is readily extendable to 2D or 3D. In particular, the extension to 2D or

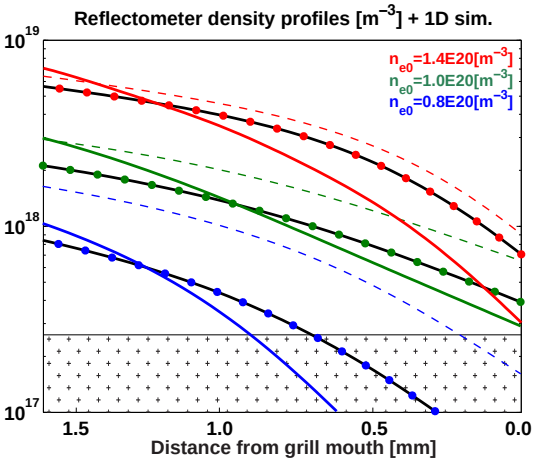

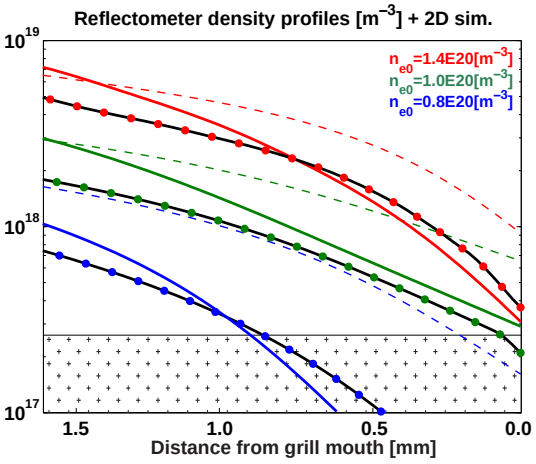

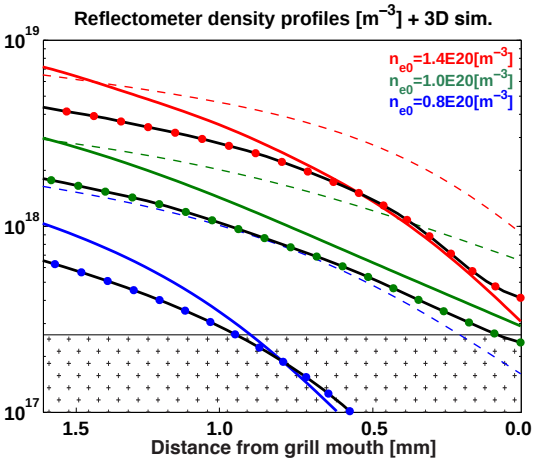

Figure 8. 1D, 2D and 3D simulation of ponderomotive forces starting from reflectometer profiles. Dashed and solid lines represent the measured profile for *LH off* and *LH on*, respectively. Black lines with colored dots represent the density profile as calculated at final stage of the POND simulation.

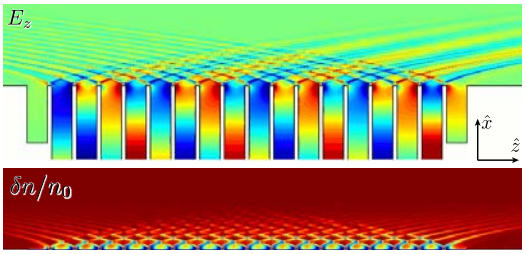

Figure 9. The electric field Re{E_z} (A), and density depletion $\delta n=(n_e-n_{e0})/n_{e0}$ (B) are shown at the first step of the iteration of the 2D simulation corresponding to the low density case.

3D allows more physics to be taken into account, namely the effect of a realistic $n_{||}$ spectrum and the inclusion of higher order modes at the waveguides' openings (in view of the 2D nature of the model only modes which have no poloidal ($\hat{y}$) variations can exist (TEM, TM and TE_{x0}, which however are the ones known to have the largest contribution [16]). The simulation results of the first iteration step of a 2D simulation corresponding to the low density discharge are shown in Fig. 9. In this simulation a grill composed of 16 active and two passive waveguides launches LH waves into the plasma. Other effects which were not (but could be) considered for this analysis are **B** tilt, curvatures, and poloidal/toroidal non-uniformities.

Figure 9(A) shows the Re{E_z} component of the waves electric field along the magnetic field direction. The most striking feature of this picture are the resonance cones (main lobe going right, high $n_{||}$ reverse lobes going to the left) that the wave forms inside of the plasma. An artificial damping term is used close to the boundaries of the plasma, away from the launcher, to avoid reflection at the boundaries of the simulation domain. Also visible are the higher order waveguide modes which are excited at the interface between the grill and the plasma. These modes are highly evanescent and decay fast for distances longer than the waveguide openings. The passive waveguides at each side of the launcher reflect the power which is coupled through the plasma with the addition of a phase difference of 90 degrees. Under the assumption that most of the power comes from the adjacent waveguide, the phasing of this waveguide is therefore consistent with a 90 degree phased waveguide array. This wave field results in the density depletion $\delta n=(n_e-n_{e0})/n_{e0}$ depicted in Fig. 9(B). A striking difference in respect with the 1D simulation results is that the density depletion is enhanced by the standing wave pattern of the resonance cones in front of the grill. This effect is the result of considering a realistic $n_{||}$ spectrum

to be launched into the plasma. By contrast, in the 1D simulation all of the power was assumed to be in a single $n_{\|}$ component of the spectrum. In view of the non-linear nature of the ponderomotive problem, this effect can not be simply reproduced by superimposing several 1D solutions with different $n_{\|}$.

5. Conclusions

The final outcome of this extensive analysis in agreement with existing work [14, 3, 7]. The density depletion measured in front of the launcher is compatible with the effect induced by ponderomotive forces of LH waves. The innovative modeling method used in the POND code and the availability of SOL density depletion profiles have allowed an unprecedented strong validation of the ponderomotive theory.

Finding methods for controlling the electron density in front of the coupler are ultimately needed to obtain good coupling. The results presented in this paper have driven the design of a new set of LH launcher private limiters for the Alcator C-Mod coupler, which will allow to access higher density/temperature regions in the SOL plasma, the hope being to reducing the effect of ponderomotive forces and broaden the antenna range of operations.

Future work in this area includes using the predictive capability of the POND model to simulate the effect of ponderomotive forces for other LHCD experiments, and in particular for ITER, which is expected to operate at high power densities. From a modeling point of view, 2D/3D effects (such as **B** tilt, curvatures, poloidal/toroidal non-uniformities) which were not considered for this analysis could be also studied. In addition, the POND code may be extended to investigate the vortex structures which are routinely observed on the visible camera diagnostic on Alcator C-Mod and other devices during high power operation. Since their structure is inherently 3D, the FEM approach and the iteration scheme used by POND might be easily adapted to include the additional physics that has been proposed to explain this phenomena [13]. Finally, the POND code would be the perfect candidate to study fast particle generation in front of LH grills. Following the approach of Ref. [18], the POND code should be modified to include the effect of electron Landau damping, which could be done using the same procedure used in the LHEAF code [19].

6. References

1. Brambilla, M., Nuclear Fusion, 1979, **19**, 1343-1357
2. Leuterer, F. et al., Plasma Physics and Controlled Fusion, Institute of Physics Publishing, 1991, **33**, 169-180
3. Fukuyama, et al., Plasma Physics, Institute of Physics Publishing, 1980, **22**, 565-578
4. Stevens, J. et al., Nuclear Fusion, 1981, **21**, 1259-1264
5. Jaquet, P. et al., AIP Conference Proceedings, 1996, **355**, 122-125
6. Bell, R. et al., Nuclear Fusion, IOP Publishing, 1994, **34**, 271
7. Petrzilka, V. et al., Czechoslovak Journal of Physics, Springer Netherlands, 1983, **33**, 1002-1010
8. Goniche, M. et al., Nuclear Fusion, IAEA, 1998, **38**, 919-937
9. Meneghini, O. et al., AIP Conference Proceedings, AIP, 2009, **1187**, 423-426
10. Hanson, G. et al., Review of Scientific Instruments, 2008, **79**, 10F114
11. Lau, C. et al., AIP Conference Proceedings of 19th Topical Conference on Radio Frequency Power in Plasmas, AIP, 2011 (to be bublished)
12. Petrzilka, V. et al., Nuclear fusion, IOP Publishing, 1991, **31**, 1758
13. Motley, R. et al., Physics of Fluids, 1980, **23**, 2050
14. Chan, V. et al., Physics of Fluids, 1979, **22**, 1724
15. Carry, J. et. al., Phys. Rev. Lett., American Physical Society, 1977, **39**, 402-404
16. Hillairet, J. et al., Nuclear Fusion, 2010, **50**, 125010
17. Ekedahl, A. et al., AIP Conference Proceedings, AIP Conference Proceedings, 2009, **1187**, 407
18. Petrzilka, V. et al., Plasma Physics and Controlled Fusion, 2011, **53**, 054016
19. Shiraiwa, S. et al., Physics of Plasmas, 2010, **17**, 056119

7. Acknowledgements

Work supported by USDOE awards DE-FC02-99ER54512 and DE-AC02-76CH03073.